nature immunology

The CDR3 regions of an immunodominant T cell receptor dictate the 'energetic landscape' of peptide-MHC recognition

Natalie A Borg[1,4], Lauren K Ely[1,4], Travis Beddoe[1], Whitney A Macdonald[1], Hugh H Reid[1], Craig S Clements[1], Anthony W Purcell[2], Lars Kjer-Nielsen[2], John J Miles[3], Scott R Burrows[3], James McCluskey[2] & Jamie Rossjohn[1]

The energetic bases of T cell recognition are unclear. Here, we studied the 'energetic landscape' of peptide–major histocompatibility complex (pMHC) recognition by an immunodominant αβ T cell receptor (TCR). We quantified and evaluated the effect of natural and systematic substitutions in the complementarity-determining region (CDR) loops on ligand binding in the context of the structural detail of each component of the immunodominant TCR-pMHC complex. The CDR1 and CDR2 loops contributed minimal energy through direct recognition of the antigen and instead had a chief function in stabilizing the ligated CDR3 loops. The underlying energetic basis for recognition lay in the CDR3 loops. Therefore the energetic burden of the CDR loops in the TCR-pMHC interaction is variable among TCRs, reflecting the inherent adaptability of the TCR in ligating different ligands.

The specificity of the cellular immune responses is determined mostly through the clonally distributed αβ T cell antigen receptors (TCRs) that 'co-recognize' structural determinants on peptides in complex with products of the major histocompatibility complex (pMHC)[1]. The atomic detail of the TCR-pMHC interactions permits several generalizations to be made regarding the nature of TCR engagement of the pMHC complex[2–14]. The emerging paradigm of TCR recognition suggests a common diagonal docking mode that may be an important factor in coreceptor ligation or signalling[15–17]. In this diagonal framework, the complementarity-determining region 1 (CDR1) and CDR2 loops of the TCR contact the MHC α-helices, whereas the hypervariable CDR3 regions interact mainly with the peptide, although variations on these generalities have been reported[17].

Those structural investigations have been complemented by an evaluation of the biophysical basis of the TCR-pMHC interaction. Such studies, using surface plasmon resonance and calorimetry approaches, showed the TCR-pMHC interaction to be dominated by weak intermolecular interactions (low micromolar range), with slow association rates and fast dissociation rates[18]. The slow association rates are consistent with the conformational plasticity of the CDR loops that was noted after pMHC engagement. Evidence so far suggests the TCR-pMHC interaction is enthalpically driven (heat is lost)[19,20] and order is imposed (entropic penalty), which is consistent with the reported inherent flexibility of the TCR CDR loops' being stabilized after pMHC ligation. The biological outcome of TCR engagement is considered to be related to the half-life and heat capacity changes of the complex[19–22].

To probe the nature of the TCR-pMHC engagement further, alanine-scanning mutagenesis has been done in three systems: the MHC class I–restricted mouse 2C system[23,24], the MHC class II I-E^k-2B4 (ref. 25) and the MHC class I–restricted A6 TCR[26]. The 2C system involved substitutions in the TCR, whereas the other two systems involved substitutions in the pMHC. The 2C studies showed that although residues in each V_α and V_β CDR are important for binding, the most important energetic interaction is contributed by CDR1 and CDR2 (refs. 23,24). Studies of the I-E^k–moth cytochrome C system suggested a two-step mechanism for TCR recognition of the pMHC complex, whereby MHC contacts dictate the initial association, followed by peptide-mediated contacts dominating stabilization of the TCR-pMHC complex[25]. Mutational studies of the A6 TCR system showed a small region or 'hotspot' of the α1 helix that provides most of the interactions vital for TCR recognition[26]. Biophysical and structural data suggest that relatively rigid CDR1 and CDR2 loops are principally involved in stabilizing the initial association, whereas the malleable CDR3 loops stabilize the peptide contacts, enabling T cell triggering[25,26].

[1]The Protein Crystallography Unit, Monash Centre for Synchrotron Science, Department of Biochemistry and Molecular Biology, School of Biomedical Sciences, Monash University, Clayton, Victoria 3800, Australia. [2]Department of Microbiology & Immunology, University of Melbourne, Parkville, Victoria 3010, Australia. [3]Cellular Immunology Laboratory, Queensland Institute of Medical Research, Brisbane, QLD 4029, Australia. [4]These authors contributed equally to this work. Correspondence should be addressed to J.M. (jamesm1@unimelb.edu.au) or J.R. (jamie.rossjohn@med.monash.edu.au).

Published online 9 January 2005; doi:10.1038/ni1155

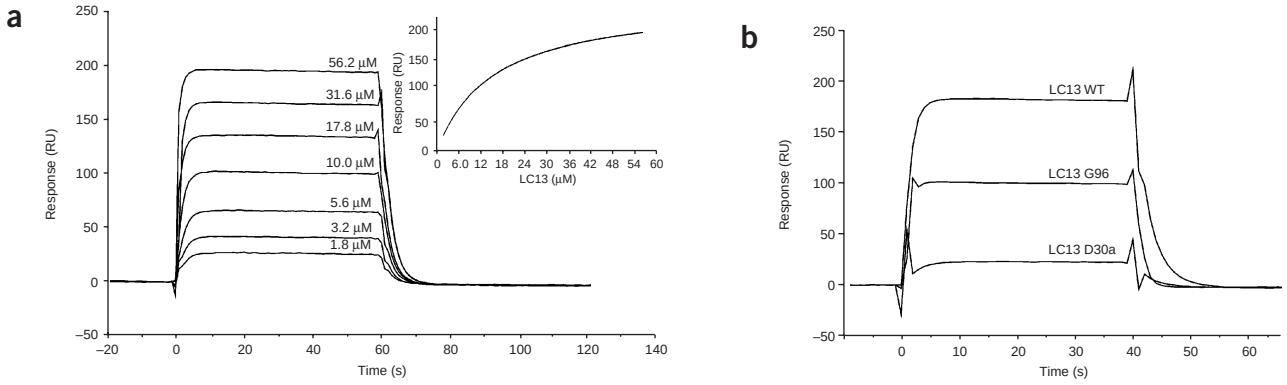

Figure 1 Binding analysis of LC13 TCR Ala point mutants to FLR–HLA-B8 by surface plasmon resonance. (**a**) Concentration series for affinity and kinetic constants measurements showing the binding of LC13 S25αAla mutants to FLR–HLA-B8; inset, equilibrium concentration–response relationship. (**b**) Comparative response of the binding of 31.6 μM LC13 wild-type (WT), LC13 G96αAla (G96) and LC13 D30AαAla (D30a) to FLR–HLA-B8.

Although the potential repertoire of TCRs is vast[27], some immune responses, for example the immune response to Epstein-Barr virus (EBV), show strong biases in TCR selection[28–30]. Unrelated people with HLA-B8$^+$ (B*0801) all make an immunodominant cytotoxic T lymphocyte response to the peptide FLRGRAYGL (FLR) derived from the latent EBV nuclear antigen (EBNA3)[28]. Structural analyses of T cell immunodominance in the immune response to infection with EBV[13] or influenza[14] have demonstrated the unique molecular properties of the immunodominant TCRs that confer specificity. However, the energetic contribution of the structural elements that govern the immunodominant TCR-pMHC interaction was not clear from those studies. To determine whether the emerging rules of engagement in TCR-pMHC interactions apply to an immunodominant TCR, we undertook binding studies and accompanying biochemical analyses of 39 mutants of the immunodominant TCR LC13, which recognizes FLR–HLA-B8. Our data show that residues in strictly conserved germline- and nongermline-encoded regions of the CDR3 loops dictate the stabilization of the complex. Thus, the energetic basis of TCR-pMHC interaction for this immunodominant TCR differs from that previously noted and demonstrates plasticity in the energetic contribution of the CDRs in TCR-pMHC ligation.

RESULTS

Rational selection and characterization of LC13 mutants

Crystal structures of the LC13 TCR and FLR–HLA-B8 alone and in complex have provided detailed insight into the structural basis of recognition[13,31,32]. However, those data did not indicate which LC13 TCR residues make crucial energetic contributions to binding. Therefore, we targeted LC13 TCR residues for substitution based on the previously determined crystal structures[13,32]. We targeted for mutagenesis the residues in the LC13 TCR that interacted with the FLR–HLA-B8 or that underwent conformational change after ligation or were exposed to solvent on a CDR loop. Accordingly, apart from two framework residues (His33α and His48α) that were involved in binding to the FLR–HLA-B8 complex, all substitutions were restricted to the CDR loops of the LC13 TCR. In total, 40 amino acids were substituted to an alanine, with the exception of alanine residues, which were substituted to glycine. The altered LC13 TCR residues were as follows: in CDR1α, Ser25, Thr26, Ser28, Thr30, Asp30A and Tyr31; in CDR2α, Leu50, Thr51, Ser52 and Asn54; in CDR3α, Pro93, Leu94, Ala95, Gly96, Gly97, Thr98, Ser99, Tyr100, Gly102, Lys103 and Leu104; in CDR1β, Ser27, Gly28, Val30 and Ser31; in CDR2β, Gln50, Asn51 and Glu52; and in CDR3β, Ser94, Ser95, Leu96, Gly 97, Gln98, Ala99, Tyr100, Glu105, Gln106 and Tyr107 and the two framework residues, His33α and His48α. Of the 40 recombinant receptors with different single-residue substitutions, only one, Leu104αAla (V_αLeu104 → Ala104), did not express and refold.

We verified the structural integrity of the refolded LC13 TCR mutants in two ways. First, we compared the solubility, yield and chromatographic activity of each receptor mutant with that of the native, refolded LC13 TCR. Second, we tested the reactivity of all receptors to an LC13 TCR monoclonal antibody (mAb; specificity, **Supplementary Figs. 1–3** online). Compared directly with the native LC13 TCR, all mutant proteins, except for His33αAla and Ser52αAla, had overlapping gel filtration and ion-exchange profiles and identical motilities by reducing and nonreducing SDS-PAGE. Moreover, all the mutant proteins reacted strongly with the LC13 mAb as did the wild-type TCR (data not shown). The yields of the purified, refolded LC13 TCR mutant proteins were also comparable to that of the typical yield of the native LC13 TCR, with 24 LC13 TCR mutants showing a similar recovery (more than 75%). Ten mutant proteins produced a moderate recovery (40–75%) and six LC13 TCR mutant proteins gave a relatively low yield (less than 40%), with the lowest recovery being that of 22% for the Gln50βAla mutant. However, we obtained sufficient quantities for the low-yielding LC13 TCR mutants for detailed surface plasmon resonance analyses. For all the mutant LC13 TCRs that were folded, none had a stability problem, as assessed by mAb reactivity (data not shown).

Surface plasmon resonance studies of the LC13 mutants

We assayed the alanine substitutions for binding to recombinant FLR–HLA-B8 using surface plasmon resonance. Measurements for the LC13–FLR–HLA-B8 interaction yielded the following values: equilibrium binding constant (K_{deq}), 12.53 μM; kinetic binding constant (K_{dcalc}), 12.30 μM; association constant (K_{ass}), 34,755 per molar per second; and dissociation constant (K_{diss}), 0.39 per second (**Fig. 1** and **Table 1**). Using the same technique, we measured the affinity of the LC13 TCR for an antagonist complex (FLRGRFYGL-HLA-B8, where P7Y is substituted with F (underlined)) as 138 μM and for a weak agonist complex (FLRGRAFGL-HLA-B8) as 113 μM (data not shown). Given that the FLRGRFYGL-HLA-B8 antagonist complex had a change in free energy (ΔΔG) of 1.42 kcal/mol and the FLRGRAFGL-HLA-B8 weak agonist complex had a ΔΔG value of 1.33 kcal/mol (data not shown), these values emphasize the small energetic

Table 1 The effect of defined substitutions on LC13 ligand binding

Residue	K_{deq} (μM)	K_a ($\times 10^4$ per molar per second)	K_d (per second)	$t_{1/2}$[a] (s)	$\Delta\Delta G_{eq}$[b] (kcal/mol)	FLR–HLA-B8 contacts	Effect on affinity
WT	12.5 ± 2.1	3.48 ± 0.75	0.39 ± 0.020	1.78 ± 0.11	–	–	–
CDR1α							
S25	14.8 ± 0.55	2.41 ± 0.35	0.37 ± 0.006	1.88 ± 0.03	0.1 ± 0.02	N	*
T26	19.4 ± 0.55	4.04 ± 0.29	0.49 ± 0.002	1.43 ± 0.004	0.26 ± 0.02	N	*
S28	11.7 ± 0.85	4.12 ± 0.29	0.40 ± 0.019	1.75 ± 0.08	−0.04 ± 0.04	Y	*
T30	33.7 ± 1.2	1.63 ± 0.015	0.66 ± 0.050	1.06 ± 0.04	0.58 ± 0.02	Y	**
D30A	>200	ND	ND	ND	>1.64	N	***
Y31	26.7 ± 4.2	ND	ND	ND	0.45 ± 0.09	Y peptide	**
Framework residues							
H33	>200	ND	ND	ND	>1.64	Y	***
H48	82.4 ± 2.9	0.54 ± 0.10	0.56 ± 0.075	1.26 ± 0.08	1.12 ± 0.02	Y	***
CDR2α							
L50	>200	ND	ND	ND	>1.64	Y	***
T51	4.87 ± 0.09	3.43 ± 0.020	0.23 ± 0.016	3.09 ± 0.21	−0.56 ± 0.01	N	*
S52	28.2 ± 2.2	1.09 ± 0.12	0.25 ± 0.018	2.84 ± 0.20	0.48 ± 0.05	N	**
N54	12.1 ± 0.45	2.61 ± 0.35	0.29 ± 0.017	2.37 ± 0.13	−0.02 ± 0.02	N	*
CDR3α							
P93	>200	ND	ND	ND	>1.64	N	***
L94	>200	ND	ND	ND	>1.64	Y peptide	***
A95	34.9 ± 3.6	ND	ND	ND	0.61 ± 0.06	N	**
G96	45.4 ± 4.2	ND	ND	ND	0.76 ± 0.05	Y	**
G97	>200	ND	ND	ND	>1.64	Y	***
T98	61.4 ± 4.8	ND	ND	ND	0.94 ± 0.05	Y	***
S99	50.5 ± 0.8	ND	ND	ND	0.83 ± 0.01	Y	***
Y100	>200	ND	ND	ND	>1.64	Y	***
G102	>200	ND	ND	ND	>1.64	N	***
K103	>200	ND	ND	ND	>1.64	N	***
CDR1β							
S27	13.2 ± 1.0	2.89 ± 0.14	0.41 ± 0.047	1.72 ± 0.20	0.03 ± 0.04	N	*
G28	7.67 ± 0.06	3.53 ± 0.43	0.41 ± 0.070	1.72 ± 0.29	−0.29 ± 0.001	N	*
V30	20.5 ± 1.3	ND	ND	ND	0.29 ± 0.04	N	*
S31	75.3 ± 1.1	ND	ND	ND	1.06 ± 0.01	Y	***
CDR2β							
Q50	11.1 ± 1.4	3.45 ± 0.005	0.47 ± 0.021	1.49 ± 0.07	−0.07 ± 0.07	Y	*
N51	6.02 ± 1.5	2.21 ± 0.32	0.19 ± 0.005	3.62 ± 0.09	−0.43 ± 0.15	Y	*
E52	49.8 ± 4.3	ND	ND	ND	0.82 ± 0.05	Y	**
CDR3β							
S94	20.8 ± 1.1	2.40 ± 0.015	0.53 ± 0.064	1.32 ± 0.16	0.3 ± 0.03	N	*
S95	4.45 ± 0.30	3.10 ± 0.095	0.15 ± 0.002	4.52 ± 0.04	−0.61 ± 0.04	N	*
L96	15.2 ± 1.0	2.35 ± 0.53	0.40 ± 0.007	1.75 ± 0.03	0.11 ± 0.04	Y	*
G97	>200	ND	ND	ND	>1.64	Y	***
Q98	>200	ND	ND	ND	>1.64	Y peptide	***
A99	>200	ND	ND	ND	>1.64	Y peptide	***
Y100	>200	ND	ND	ND	>1.64	Y peptide	***
E105	15.3 ± 1.2	2.12 ± 0.28	0.44 ± 0.050	1.61 ± 0.17	0.12 ± 0.04	N	*
Q106	>200	ND	ND	ND	>1.64	N	***
Y107	19.4 ± 0.7	2.42 ± 0.16	0.53 ± 0.055	1.32 ± 0.14	0.26 ± 0.02	N	*

[a]$t_{1/2} = 0.693/kd$. [b]$\Delta\Delta G = RT\ln(K_{dmut}/K_{dWT})$, where R is the gas constant and T is the temperature in Kelvin. mut, mutant; WT, wild type; *, less than twice the wild-type value; **, less than four times the wild-type value; ***, four times or more the wild-type value. ND, not determined; Y, Yes; N, no.

differential for signaling or nonsignaling outcomes for this immunodominant TCR.

We determined the K_{deq} of the interaction for the 39 LC13 TCR substitutions (**Figs. 1** and **2**, **Table 1** and **Supplementary Figs. 1–3** online) and measured the kinetic rate constants of the interaction for approximately half of the LC13 TCR mutants that had a K_{deq} of less than 100 μM (**Table 1** and **Supplementary Figs. 1–3** online). No mutant had a K_{deq} of between 100 and 200 μM. However, we recorded many K_{deq} values above 200 μM (**Table 1** and **Supplementary Figs. 1–3** online). We consider a K_{deq} above 200 μM as approaching the upper limit of reasonably accurate estimations for affinity in this system and so we designated any K_{deq} value for the LC13 mutants above 200 μM as being greater than 200 μM. In all cases, the K_d calculated from the kinetic data matched the K_d estimated from the equilibrium data, emphasizing the internal consistency of the data and indicating that that there were no mass transport effects at the concentration of the reagents used. We considered the substitutions as having a small effect on the interaction if the K_{deq} for the mutant was less than twofold, an intermediate effect if the K_{deq} for the mutant was between two and fourfold, and a notable effect if the K_{deq} was more than fourfold compared with the K_{deq} of the native LC13-FLR–HLA-B8 interaction (**Table 1** and **Fig. 2**).

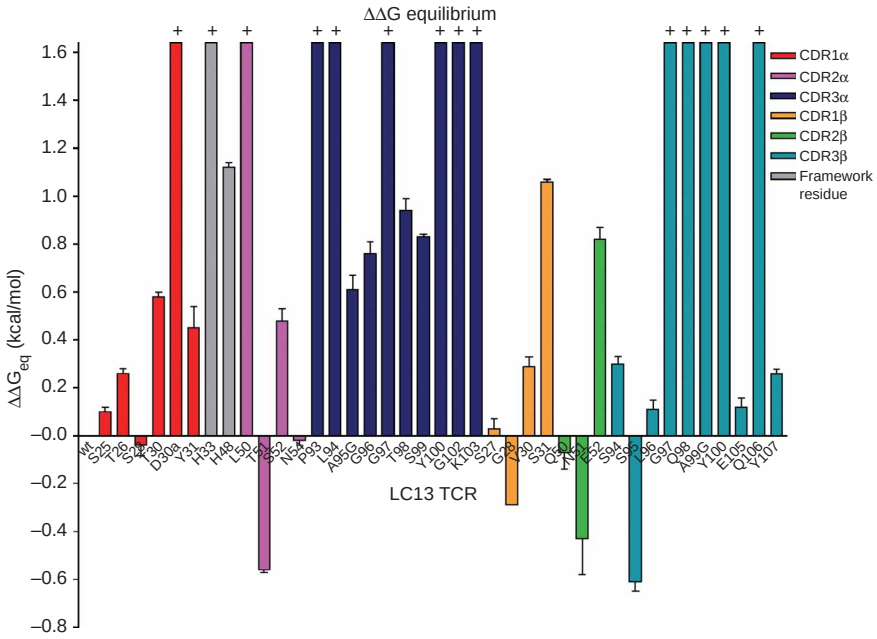

Figure 2 Effect of substitutions on the LC13–FLR–HLA-B8 interaction. Change in energy (ΔΔG$_{eq}$) associated with the ligation of the LC13 TCR with FLR–HLA-B8 for the 39 LC13 TCR mutants generated. Larger positive values indicate less-favorable binding energy than that of wild-type. Error bars represent the standard error of replicate experiments.

Structural perspectives

Structures have been determined to a resolution of 1.8 Å for nonliganded FLR–HLA-B8 (ref. 31), to a resolution of 1.5 Å for nonliganded LC13 TCR[32] and to a resolution of 2.5 Å in complex with FLR–HLA-B8 (ref. 13). After ligation, the buried surface area (BSA) of the LC13 TCR was approximately 1,100 Å^2 with the CDR1α, CDR2α, CDR3α and CDR3β loops undergoing considerable conformational changes. All the CDR loops of the LC13 TCR were in contact with FLR–HLA-B8, with the CDR1β loop contributing 4% BSA (1% contacts); CDR1α, 17% BSA (15% contacts); CDR2α, 17% BSA (4% contacts); CDR2β loops, 17% BSA (17% contacts); CDR3β loop, 21% BSA (37% contacts); and CDR3α loop, 24% BSA (25% contacts) at the interface. In the complex with ligand, four residues from CDR1α and no residues from CDR2α interacted with CDR3α; whereas three residues from CDR1β and no residues from CDR2β interacted with CDR3β.

Effect of CDR1β mutants

Given that CDR1β interacts marginally with FLR–HLA-B8, it was not unexpected that three of the four substituted residues in CDR1β had little effect on recognition (**Table 1** and **Fig. 3a**). However, the Ser31βAla substitution had a considerable effect on the interaction (ΔΔG, 1.06 kcal/mol). At first, this result seemed to represent an anomaly; the Ser31β side chain formed one van der Waals contact, with a residue on the α1 helix of HLA-B8 (**Fig. 3a**), yet substitution of this residue to Ala resulted in a substantial reduction in affinity (**Table 1**). Although the CDR1β loop did not change conformation after binding to FLR–HLA-B8, the CDR3β loop was repositioned such that it then was in contact with the CDR1β loop. The only contact formed between CDR1β and CDR3β loops was mediated through the Ser31β$^{O\gamma}$ group, where it formed hydrogen bonds onto Gln98β^{N} of the CDR3β loop (**Fig. 3a**). Accordingly, the structural and surface plasmon resonance data suggest that Ser31β is essential in stabilizing the ligated conformation of the CDR3β loop. This finding supports observations made with the 2C TCR, for which CDR1β residues that were not in contact with antigen still contributed substantially to binding energy through stabilization of the CDR3β loop[23].

Effect of CDR1α mutants

The CDR1α loop interacted at discrete sites on the FLR–HLA-B8 complex, contacting Arg62 of the α1 helix and a stretch of the α2 helix (residues 151–155) as well as the antigenic peptide (**Fig. 3b**). Three of the six LC13 TCR mutants in the CDR1α loop had a small effect on the recognition of FLR–HLA-B8 (**Table 1** and **Fig. 3b**). The Ser25α and Thr26α side chains did not contact FLR–HLA-B8 and so their negligible effect on ligand recognition was predicted. However, Ser28α formed hydrogen bonds to Arg62 (**Fig. 3b**) and, given the apparent importance of the polymorphic Arg62 residue in ligating the CDR1α loop in all known TCR complexes[33], it was unexpected that the Ser28αAla replacement had little effect on recognition (**Table 1**). However, Arg62 also formed a water-mediated hydrogen bond with the Thr26α main chain (**Fig. 3b**) and so we could not conclusively rule out a precise energetic function for Arg62 ligation here. Although Tyr31α formed van der Waals contacts with the aromatic ring of the P7-Tyr (FLR peptide residue 7) that is essential to the specificity of the LC13 TCR and also formed hydrogen bonds onto HLA-B8 (**Fig. 3b**), the Tyr31αAla substitution had only a moderate effect on ligand recognition (**Fig. 2** and **Table 1**). Conversely, neither the Thr30α nor the Asp30Aα side chains interacted with FLR–HLA-B8, yet the Thr30αAla substitution had a moderate effect on recognition, whereas the Asp30AαAla substitution had a profound effect on recognition (**Table 1** and **Fig. 2**). The structural basis of the effect of these

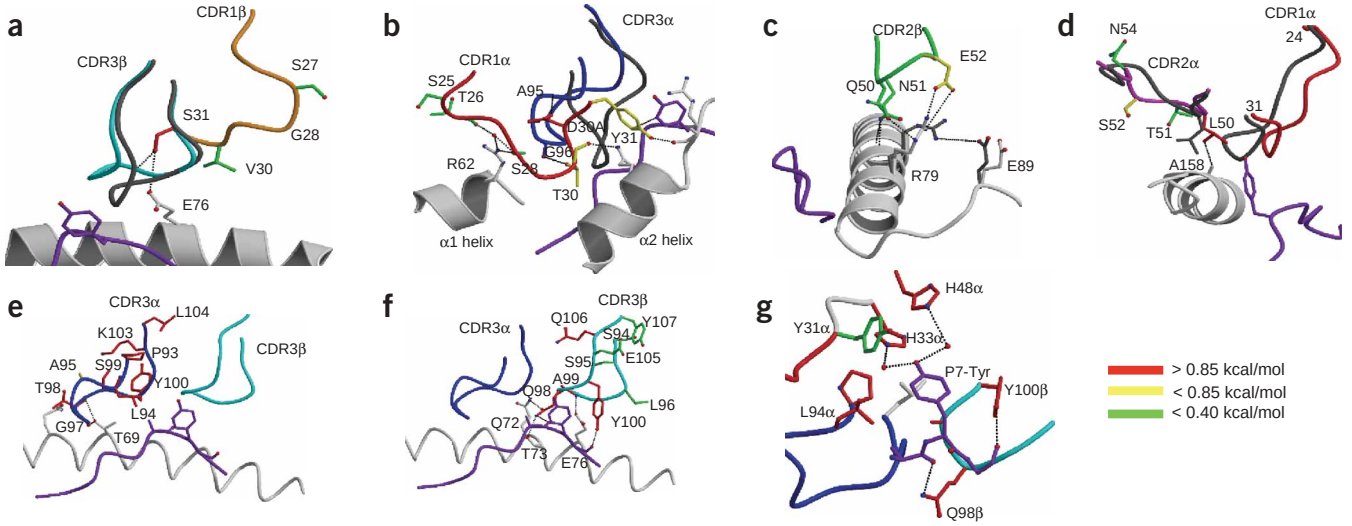

Figure 3 LC13 TCR residues that are essential for interaction with FLR–HLA-B8. CDR loops: CDR1α, red; CDR3α, blue; CDR1β, orange; CDR3β, cyan. Interactions, dotted lines; non-liganded conformations, dark gray; HLA-B8, light gray; peptide, purple. LC13 TCR residues are assigned colors according to energetic contribution (key). (**a**) Ser31 of CDR1β stabilizes the ligated conformation of the ligated CDR3β loop. (**b**) CDR1α loop interactions with the CDR3α loop and HLA-B8. (**c**) The polar contacts mediated through the CDR2β loop. (**d**) Comparison of the conformations of CDR2α loop with and without ligand formation. (**e**) CDR3α interactions with HLA-B8. (**f**) CDR3β loop interactions with HLA-B8 and the FLR peptide. (**g**) Interaction of the framework residues (His33 and His48) with the FLR peptide.

substitutions was apparent when we compared the non-liganded and liganded conformations of the LC13 TCR (**Fig. 3b**). In the non-liganded state, the CDR1α loop did not interact with the other CDR loops; however, after binding, the CDR3α loop shifted forward and contacted residues 28–32 of the CDR1α loop (**Fig. 3b**). The Thr30α and Asp30Aα residues were the sole residues from the CDR1α loop that mediated contacts with the ligated CDR3α loop, with Thr30α forming hydrogen bonds to Gly96α^{O} and Asp30Aα forming hydrogen bonds onto the main chain of Ala95α and Gly96α (**Fig. 3b**). Thus, the CDR1α loop is essential in stabilizing the conformation of the ligated CDR3α loop, analogous to the function of CDR1β in stabilizing CDR3β discussed above.

Effect of CDR2β mutants

The CDR2β loop contained many polar side chains (Gln50β, Asn51β and Glu52β) that interacted extensively with a localized stretch of the HLA-B8 α1 helix (residues 72–79; **Fig. 3c**). Nevertheless, substitutions in the CDR2β loop had a modest effect on recognition. For example, despite the fact that Gln50β formed two hydrogen bonds with HLA-B8, the Gln50βAla mutant showed a small change in ΔΔG (**Fig. 3c** and **Table 1**). Moreover, the Asn51βAla substitution improved the affinity of the interaction (discussed later). The Glu52βAla substitution, which would disrupt the only salt bridge at the interface, did have a moderate effect on the interaction (**Table 1**). To form the Glu52β-Arg79 interaction after TCR ligation, Arg79 has to break a salt bridge with Glu89 of HLA-B8, and this may have offset the favorable energetic contribution normally associated with salt bridge formation (**Fig. 3c**). Collectively, the energetic contribution of the CDR2β loop was unexpectedly small.

Effect of CDR2α mutants

Three of the four residues that were substituted in the CDR2α loop (Thr51α, Ser52α and Asn54α) were not in contact with the antigen, with Thr51α and Asn54α minimally affecting recognition (**Table 1** and

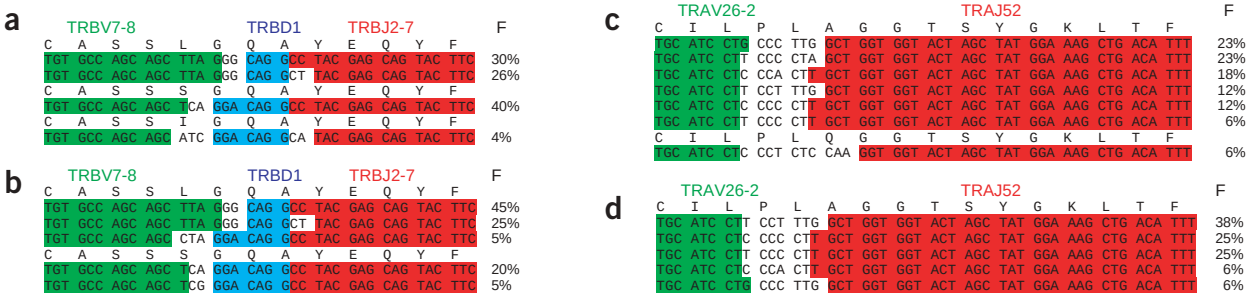

Figure 4 Natural variation in 'public' TCR sequences used in the HLA-B8-restricted, FLR-specific antiviral CD8$^+$ T cell response. Nucleotide and amino acid sequences of natural TRBV7-8 and TRAV26-2 CDR3 chains isolated from bone marrow donor volunteers. FLR-specific CD8$^+$ T cell populations were expanded and were sorted with an HLA-B0801-FLRGRAYGL multimer (**a**,**c**) or a mAb specific for the TRBV7-8 'public' TCR (**b**,**d**). DNA from each pool of sorted cells was amplified with TRBV7 primers (**a**,**c**) and TRAV26 primers (**b**,**d**) and the products were cloned into bacteria. Many bacterial clones were sequenced; F (far right) indicates the frequency of a particular chain. Green, V_α or V_β family germline nucleotides; blue, TRBD (β-chain diversity segment) germline nucleotides; red, J_α or J_β (joining region family) germline nucleotides.

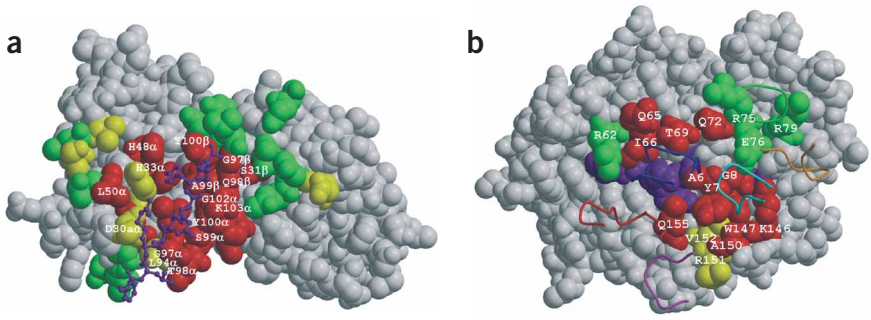

Figure 5 The LC13 TCR and HLA-B8 hotspot. (**a**) Surface representation of the LC13 TCR in the liganded state. TCR residues are assigned colors according to the effect of their substitution on binding to FLR–HLA-B8. Residues that weakened the affinity by at least fourfold are red; by fourfold, yellow; by twofold, green. FLR peptide (presented for reference) is purple. (**b**) Surface representation of the conformation of FLR–HLA-B8 with ligand demonstrating residues that make substantial contact with the LC13 TCR. Contact residues are assigned colors according to the effect that LC13 TCR substitution has on binding to FLR–HLA-B8 (as in **a**). FLR–HLA-B8 residues that are in contact with more than one LC13 TCR residue have been assigned colors according to the most important effect noted. The FLR peptide is in purple except for important contact residues; those residues have been labeled.

Fig. 3d). In contrast, the Ser52αAla showed a moderate effect on recognition, which seems to correspond to a function for Ser52α in stabilizing the conformation of the CDR2β loop in the state without ligand formation (**Table 1** and **Fig. 2**). The Leu50αAla substitution had a considerable effect on the interaction with FLR–HLA-B8 (**Fig. 2**). Leu50α interacted directly with HLA-B8; however, the effect of this Leu50αAla substitution was disproportional to the extent of contact, as it formed only a single van der Waals interaction with HLA-B8 (Leu50α$^{C\delta2}$ interacted with Ala158$^{C\beta}$; **Fig. 3d**). The structural analyses suggest that Leu50α has a principal function in stabilizing the ligated conformation of the CDR1α loop, where it makes van der Waals contacts with the main chains of the CDR1α C-terminal residues (Gly29α, Thr30α and Asp30Aα), as well as the side chain of Tyr31α.

Effect of CDR3α mutants

We made 11 substitutions in the CDR3α loop in the region between Pro93α and Leu104α, the two residues that defined the pivot points of conformational change that occurred in this loop after ligation (**Table 1** and **Fig. 3e**). The Leu104αAla mutant could not be refolded, emphasizing the important structural function this residue has in LC13 TCR stability. Eight of the ten substitutions had a profound effect on recognition (**Table 1** and **Figs. 2** and **3e**). The side chains of Leu94α, Thr98α and Tyr100α were in contact with FLR–HLA-B8 and the substantial effect of their substitutions was directly related to a loss of specificity-governing interactions (**Fig. 3e**). Ala95α and Gly96α, whose substitutions had a moderate effect on recognition, mediated the interactions with the ligated CDR1α loop and thereby stabilized the conformation of the ligated CDR3α loop. The Gly96α residue was also in contact with antigen (along with Gly97α), so some of the effect of these substitutions must also reflect this function. The CDR3α loop contains three Gly residues, suggesting that structural plasticity of the CDR3α loop is essential for antigen recognition. Pro93α is a nongermline-encoded residue that does not contact the antigen, yet, as judged by the effect of the Pro93αAla substitution (**Table 1**), seems to represent a critical residue that controls the conformational dynamics of the CDR3α loop. Similarly, the effect of the Ser99αAla substitution showed that Ser99α, which formed hydrogen bonds onto Gly96α^{N}, was important in stabilizing the conformation of the CDR3α loop in the unliganded state (data not shown). The effect of the Lys103αAla substitution suggests that Lys103α, which participates in intersubunit interactions, is essential in stabilizing the V_α-V_β interface. Our data establish that the CDR3α loop, which interacts mainly with the α1-helix of HLA-B8, has an essential function in the energetics of recognition of the FLR–HLA-B8 complex.

Effect of CDR3β mutants

The CDR3β loop is the principal loop of the immunodominant TCR that interacts with the FLR peptide. We made ten substitutions in the CDR3β loop and of these substitutions, five (Gly97βAla, Gln98βAla, Ala99βGly, Tyr100βAla and Gln106βAla; **Table 1** and **Fig. 3f**) had a profound effect on recognition ($\Delta\Delta G > 1.64$ kcal/mol). Ser95β, Glu105β and Tyr107β neither contact FLR–HLA-B8 nor change conformation after ligation[13], so their substitution had a negligible effect on recognition (**Fig. 3e**). Although Leu96β was in contact with the heavy chain of HLA-B8, results with the Leu96βAla substitution suggested that Leu96β was not essential in the energetics of recognition. However, Ala99β and Tyr100β formed direct contacts with the P7-Tyr group, and the effect of their substitutions demonstrated a correspondingly essential energetic function in the interaction (**Table 1** and **Fig. 3f**). Similarly, the residue Gln98β, encoded by the D_βN region, participated in interactions with V_α, the peptide and the HLA-B8 heavy chain and this was reflected in the substantial contribution of this amino acid to the energetics of antigen recognition. The CDR3β loop was essential in recognition of the FLR–HLA-B8 complex (**Table 1** and **Fig. 2**).

Effect of V_α framework residues

In addition to the substitutions in the CDR regions, we targeted two substitutions (His33αAla and His48αAla), as these amino acids are part of the germline-encoded V_α (TRAV26-2*01) that is highly selected in unrelated, EBV$^+$ people who express HLA-B8. These two residues, located deep in the central pocket of LC13, formed water-mediated hydrogen bonds with the P7-Tyr from the peptide[13] (**Fig. 3g**). The importance of these water-mediated hydrogen bonds is suggested by the 90% loss of T cell activation after P7-Tyr–to–Phe substitution of FLRGRAFGL[13] and a corresponding 90% loss in the affinity of the LC13 TCR for this HLA-B8-peptide complex (data not shown). Consistent with these observations, both of these substitutions had a profound effect on recognition, confirming the importance of these residues in the selection of the LC13 immunodominant TCR.

Natural sequence variation in LC13 TCR

To further examine the energetic landscape of binding of LC13 to FLR–HLA-B8, we evaluated the natural sequence variation in the LC13-like TCRs of two healthy, EBV$^+$, HLA-B8$^+$ donors (**Fig. 4**) as well as those reported in the literature[34,35] (**Supplementary Figs. 1–3** online). We stimulated peripheral blood mononuclear cells from each donor with the FLR peptide *in vitro* for 10 d and sorted the responding CD8$^+$ T cells with mAb specific for the BV7-8 V_β used

by LC13 (**Supplementary Figs. 1–3** online) or with a FLR–HLA-B8 multimer (**Fig. 4**). We then cloned and sequenced PCR products from BV7-8 and TRAV26-2 transcripts. In the first donor, all genes encoding TCRα and TCRβ, including diversity (D)–, joining (J)– and untemplated (N)–region sequences, were identical to the LC13 TCR clonotype; that is, immunodominant in unrelated people ('the public'; data not shown). In the second donor (**Fig. 4**), although we found multiple codon substitutions in the D-, J- and N-region junctional sequences, with few exceptions, these preserved the CDR3α residues Pro93 (three codons) and Leu94 (five codons) shown by mutagenesis to be essential for ligand binding. The only naturally tolerated substitution in CDR3α was Ala95Gln, found in a single clone (**Fig. 4**). Ala95Ser has also been reported in this 'public' TCR[34] (**Fig. 4**). Ala95α mediates interactions with the ligated CDR1α loop, stabilizing the ligated CDR3α loop, consistent with a moderate effect on recognition by the *in vitro*–altered TCR. Presumably other residues at this position can also serve this function, allowing some natural variation at this site.

In the junctional regions of TCRβ clones from donor 2 and other published sequences[34,35], the residues Gly97 (three codons), Gln98 (two codons) and Ala99 (three codons) were all conserved despite multiple codon usage. However the N-region residue 96 contained two alternate residues, Leu96Ile and Leu96Ser, in just under half the clones. CDR3β Leu96 was in contact with the heavy chain of HLA-B8, but natural variation at this site is predicted because the Leu96Ala mutant is a minor contributor to the energetics of recognition. Thus, the natural $CD8^+$ T cell repertoire toward FLR–HLA-B8 reflects the stringent conservation of residues that make important contributions to ligand binding and the natural variants of the receptor that do retain specificity confirm the location of receptor 'hotspots' and 'cold spots' defined by the mutagenesis approach.

The hotspots of interaction

Having defined the LC13 TCR residues that contact FLR–HLA-B8, and the effect of altering these residues (**Fig. 5a**), we were able to approximate a corresponding hotspot on the FLR–HLA-B8 complex. This hotspot covered the CDR3α and CDR3β–binding site only, mapping onto the P6-P8 positions of the peptide, as well as residues Gln65, Ile66, Thr69 and Gln72 from the HLA-B8 α1 helix, and residues Lys146, Ala150 and Gln155 from the α2 helix of HLA-B8 (**Fig. 5b**).

Kinetics of TCR-pMHC interaction

We determined the association and dissociation rate constants for the native LC13 TCR–FLR–HLA-B8 interaction (**Table 1** and **Supplementary Figs. 1–3** online). We attempted a phi (ϕ) analysis[25] (an approach that allows initial stabilization contributions to be ascertained) on this LC13 TCR data set; however, the extensive conformational change in the LC13 TCR meant that most of the ϕ values were outside the expected range and therefore were not valid[25]. We were able to assess the effect of 17 LC13 TCR mutants on the kinetic rate constants of the interaction (**Table 1**). All substitutions on the CDR2α loop for which we determined kinetic constants considerably increased the half-life (calculated as $0.693/K_{diss}$) of the interaction (Thr51αAla, $t_{1/2}$ = 3.09 s; Ser52αAla, $t_{1/2}$ = 2.84 s; Asn54αAla, $t_{1/2}$ = 2.37 s). In addition, the Asn51βAla substitution and the Ser95βAla substitution substantially increased the half-life of the interaction (Asn51βAla, $t_{1/2}$ = 3.62 s; Ser95βAla, $t_{1/2}$ = 4.52 s). None of the measured mutants notably increased the association rates, whereas many mutants substantially decreased (Thr30αAla, His48αAla and Ser52αAla) or moderately decreased (Asn51βAla, Ser94βAla, Leu96βAla, Glu105βAla and Tyr107βAla) the association rates (**Table 1**). The His48αAla substitution had a particularly profound effect, with a 84.5% decrease in the 'on rate' and a much less substantial change in the 'off rate'. Of these substitutions, the side chains of His48α, Asn51β and Leu96β interacted directly with FLR–HLA-B8 complex.

Some of the Ala substitutions led to a moderate improvement in affinity for this interaction (**Table 1** and **Supplementary Figs. 1–3** online), as has been reported in previous mutagenesis studies of 2C[36,37]. The Ser95βAla substitution had the most notable effect (**Table 1**). Ser95β is located in a part of the CDR3β loop that does not interact with antigen, but forms a hydrogen bond internal to this loop. The positive effect of this substitution suggests the loss of this intraloop hydrogen bond improves the flexibility of the CDR3β loop, which seems to promote the interaction with FLR–HLA-B8. Similarly, Thr51α did not interact with FLR–HLA-B8, yet the Thr51αAla substitution improved the affinity of the interaction, suggesting that the conformational plasticity noted in the CDR2α loop after ligation is an important facet in recognition (**Fig. 3d**). Asn51β formed hydrogen bonds to Arg79 of HLA-B8 (**Fig. 3c**), yet the Asn51βAla substitution enhanced the interaction with FLR–HLA-B8, suggesting that the removal of Asn51β may remove the necessity of breaking the Arg79-Glu89 salt bridge (**Fig. 3c**). Collectively, this suggests that the affinity-improving substitutions exert their effects through reducing the steric constraints on binding.

DISCUSSION

The phenomenon of T cell immunodominance has been reported in the cytotoxic T lymphocyte response to many different viral infections[38–44]. Although we have provided a structural basis for T cell immunodominance against the EBV peptide FLR[28,39], our studies did not demonstrate the energetic landscape underlying this phenomenon. We have described here a systematic scanning mutagenesis study of a TCR-pMHC system in which the precise structural components have been defined in their liganded and non-liganded states. The question arises as to whether each of the V(D)J gene segments and N regions exclusively selected in the immunodominant LC13 TCR share the energetic load of recognition through a large number of weak contacts across the interface or if there is an energetic interaction hotspot[45]. The idea of an energetic hotspot is also consistent with previous studies of TCR-pMHC recognition[23,25,26]. If an energetic hotspot dictates the LC13 TCR–FLR–HLA-B8 interaction, where would it be located and what then drives the salient sequence conservation in the six CDR loops of the LC13 TCR? Our data have established that there is indeed a hotspot, but unexpectedly it is in the CDR3α and CDR3β loops, whereas the exclusively germline-encoded CDR1 and CDR2 loops have a minor energetic function in the interaction with FLR–HLA-B8. The sum energetic contribution from each CDR loop is as follows (in descending order): CDR3α, 12.98 kcal/mol; CDR3β, 8.38 kcal/mol; CDR1α, 2.99 kcal/mol; CDR2α, 1.54 kcal/mol; CDR1β 1.09; CDR2β, 0.32 kcal/mol. These data contrast with the energetic landscape of the 2C TCR, for which the most substantial energetic contribution to the interaction arises from the CDR1 and CDR2 loops[23]. The diminished energetic function of the CDR3 loops in the 2C TCR may be attributable, in part, to their shorter CDR3 loop lengths and Gly-rich composition compared with that of the LC13 TCR. Unlike the 2C TCR, for which both CDR3 loops interact with the peptide, there is a notable division of functions between the LC13 TCR CDR3 loops, whereby the CDR3α loop is involved principally in

interacting with the HLA-B8 heavy chain and the CDR3β loop interacts with the peptide. To assume these differing functions, both CDR3 loops of the LC13 TCR undergo large-scale conformational changes that focus the energetic hotspot to the central region of the LC13 TCR. In these CDR3 loops, most residues are critically important in specificity-determining interactions and in mediating conformational change.

To accommodate the CDR3 conformational change that occurs after ligation of FLR–HLA-B8, a concerted movement of the CDR1α and CDR2α loops is essential[13]. The largest energetic function attributable to the CDR1α loop lies in stabilizing the ligated CDR3α loop. Similarly, the CDR1β loop, which has a smaller function in directly interacting with the antigen, is critical in stabilizing the ligated conformation of the CDR3β loop. Moreover, our data suggest that conformational change in the CDR2α loop after ligation assists in the remolding of the CDR1α and CDR3α loops rather than making a direct specificity contribution to binding. Unexpectedly, the CDR2β loop, despite forming multiple ionic interactions within a localized stretch on the HLA-B8 α1-helix, had the least energetic function of the CDR loops at the interface. This observation is consistent with the location of the CDR2β loop at the periphery of the interface, whereby the need to break polar bonds offsets the contribution of bond formation. Conversely, Tyr100β from the CDR3β loop and the two framework residues encoded by the V_α gene, His33α and His48α all have an essential energetic function in recognition of the P7-Tyr.

The FLR–HLA-B8 hotspot is much more extensive than that noted before in studies of HLA-A2 (refs. 26, 46, 47). The HLA-A2 hotspot corresponds with the HLA-B8 hotspot, despite polymorphism between these alleles at α1 helix residues 65 and 66. Defining the HLA-B8 hotspot also represents an important step toward understanding the alloreactivity of the LC13 TCR to HLA-B*4402. Of the 31 amino acid polymorphisms between HLA-B*0801 and HLA B*4402, six map to the antigen surface; four, onto the α1 helix (residues 80, 81, 82 and 83); and two, onto the α2 helix (residues 163 and 167). None of these residues is involved in LC13 TCR ligation of HLA B8-FLRGRAYGL, and the remaining polymorphisms are buried. This indicates that LC13 TCR binds HLA-B*4402 (refs. 48, 49) in a way similar to HLA-B8. Thus, the sequence of the allopeptide ligand is likely to be a critical determinant of the HLA B*4402 alloreactivity, whereas the main contribution of CDR3α to binding the HLA α1 helix is also a potential conserved hotspot for alloreactivity. Our studies have shown how the TCR interaction can vary its structural focus between the peptide antigen and the HLA heavy chain, depending on the available array of solvent-exposed side chains. Thus, the MHC has more extensive involvement in TCR stabilization when there is lack of prominently exposed peptide residues to contact the TCR.

Given that the CDR1 and CDR2 loops contribute minimal energy to the direct interaction with FLR–HLA-B8, a two-step mechanism in TCR recognition is not consistent with our results. One of the great mysteries of T cell recognition is that even though the TCR is immunoglobulin like, antigen recognition is highly restricted to pMHC ligands. This might be explained if TCRs have a rudimentary scanning function, as suggested by the observation that MHC class I and class II restriction correlates with particular sequences in the TCR CDR1 and CDR 2 regions[50–54], although exceptions to these patterns are reported[36]. However, the germline-encoded CDR1 and CDR2 loops of the LC13 TCR have a minimal energetic function in recognizing the FLR–HLA-B8 complex. Thus, the energetic burden of different CDR loops in TCR-pMHC interaction apparently shifts according to the nature of the ligand, emphasizing TCR adaptability in recognizing diverse ligands. This is consistent with the idea that the TCR 'footprint' shifts between conserved residues in different pMHC complexes[55].

What are the energetic principles governing the positive selection of the LC13 TCR? The nongermline-encoded regions of the LC13 TCR CDR3 loops have prominent functions in recognition. Thus, it is possible that the nongermline-encoded regions of the TCR may have a function that is as important as that of the germline regions in dictating TCR recognition and immunodominance in selection of the T cell repertoire. Some somatic alterations in antibodies that improve the affinity for the antigen also stabilize CDR loop conformation rather than directly contacting the antigen itself[56]. Thus, the evolution of antibody maturation seems to mirror the evolution of TCR recognition, which for this particular immunodominant TCR has been raised to combat the ancient EBV.

METHODS

Construction of LC13 mutants. In total, 40 amino acids were substituted to Ala, except for Ala residues, which were substituted to Gly. The original LC13 human T cell clone was prepared as described[57] and was used as the template to generate the forty LC13 mutants by site-directed mutagenesis (QuikChange; Stratagene).

Expression and purification of recombinant proteins. Soluble FLR–HLA-B8 complex was prepared from *Escherichia coli* as described[57]. The refolded complexes were concentrated and purified by anion exchange and gel filtration chromatography. The α- and β-chains of the LC13 TCR were expressed in BL21 (DE3) *E. coli* cells, refolded from inclusion bodies and purified as described[57]. The structural integrity of the refolded proteins was confirmed by the apparent molecular weight of the protein after size-exclusion chromatography and by SDS-PAGE.

Enzyme-linked immunosorbent assay (ELISA) and mAbs reactive against LC13 TCR. Two mAbs reactive to LC13 were generated 'in-house' (description, **Supplementary Figs. 1–3** online) and were used to probe the native conformation of recombinant TCRs in a capture ELISA assay. The mAb 12H8 (IgG, to C_α; 100 μl at a concentration of 10 μg/ml) was used to coat 96-well ELISA plates (U96 Maxisorp, Nunc) at 4 °C for 16 h before blocking at 37 °C for 1 h with 200 μl of 1% BSA in PBS. Positive control wild-type LC13, the mutant LC13 TCRs or the negative control TCR CF34 were then added to the wells for 1 h in triplicate at a concentration of 10, 1, 0.1 or 0.01 μg/ml. The biotinylated mAb 13G11 (IgG, to LC13 V_β) was then added at a concentration of 1 μg/ml and bound mAb was detected with horseradish peroxidase–conjugated antibody to mouse immunoglobulin (Silenus). Reaction with the substrate O-phenylenediamine substrate (Sigma) was terminated with HCl, and ELISA plates were 'read' at 492 nm on a Labsystems Multiscan ELISA plate reader.

Surface plasmon resonance measurements and analysis. All surface plasmon resonance experiments were done at 25 °C on a Biacore 3000 instrument with HBS buffer (10 mM HEPES HCl, pH 7.4, 150 mM NaCl and 0.005% surfactant P20 supplied by the manufacturer) supplemented with 1% BSA to inhibit nonspecific binding. The antibody W6/32 (ref. 58) was coupled in 10 mM citric acid, pH 5.0, to research grade CM5 chips with standard amine coupling at 9,000–11,000 resonance units (RU). For each experiment, 200–400 RU of the FLR–HLA-B8 was 'captured to' the antibody. LC13 wild-type and mutants were injected over all flow cells at a rate of 20 μl/min or more. The final response was calculated by subtraction of the response of the antibody alone from that of the antibody–HLA-B8 complex. The antibody surface was regenerated between each analyte injection with ActiSep (Sterogene). All measurements were minimally in duplicate, and where the replicates were not consistent, the measurements were repeated. All mutants were originally tested in a concentration range of 1–56.2 μM; if the binding was too weak, the concentration range was increased to 50–200 μM. BIAevaluation Version 3.1 (Biacore AB) was

used for all data analysis; the 1:1 Langmuir binding model, allowing for local fitting of the binding maximum, was used to calculate the kinetic constants. To allow for the capture system, the model was modified to include an additional parameter for the drifting baseline and local fitting of the binding maxima. The K_{dcalc} (K_{diss}/K_{ass}) concurred with the K_{deq} for all reported values.

Generation of bulk T cell cultures, sorting and TCR gene sequencing. Short-term cytotoxic T lymphocyte bulk cultures from two EBV$^+$, HLA-B8$^+$ donors were generated by culture of peripheral blood mononuclear cells (2×10^6 per 2-ml well) in growth medium with autologous peripheral blood mononuclear cells that had been precoated with FLR peptide (1 μM for 1 h; responder:-stimulator ratio, 2:1). On days 3 and 7, cultures were supplemented with recombinant interleukin 2 (20 U/ml) before sorting on day 10 with either FLR–HLA-B8R–phycoerythrin tetramer or FLR–HLA-B8R–phycoerythrin pentamer (ProImmune) or mAb 13G11 (data not shown) specific for the BV7-2 (TCR β-chain) expressed by LC13. Cells were labeled with CD8–tricolor (Caltag) and CD3-allophycocyanin (BD Pharmingen) and were sorted on a MoFlo apparatus (Cytomation).

Total RNA was extracted from bulk cultures with TRIzol reagent (Invitrogen). Reverse transcription was done with Superscript III (Invitrogen) and antisense TCRα and TCRβ chain primers[59]. PCR used a 25-μl volume containing 200 μM dNTPs, 20 mM $MgCl_2$ and 1.25 U of AmpliTaq Gold (Applied Biosystems) with a TCRα constant region primer and TRAV26 family–specific primer, or a TCRβ constant region primer and a TRBV6 family–specific primer[59]. PCR products were purified and cloned into the pGEM-T vector system (Promega) and were sequenced with the ABI PRISM Big Dye Termination Reaction Kit (Applied Biosystems).

Note: Supplementary information is available on the Nature Immunology website.

ACKNOWLEDGMENTS

The authors thank F. Carbone and A. Brooks for critically reading the manuscript, and K. Davern (The Walter and Eliza Hall Institute of Medical Research) for assistance in producing the mAbs to LC13. Supported by a Wellcome Trust Senior Research Fellowship in Biomedical Science in Australia (J.R.), the University of Melbourne (A.W.P.), National Health and Medical Research Council (Australia) and Australian Research Council, the Roche Organ Transplantation Research Foundation and the Juvenile Diabetes Research Foundation.

COMPETING INTERESTS STATEMENT

The authors declare that they have no competing financial interests.

Received 24 September; accepted 8 December 2004
Published online at http://www.nature.com/natureimmunology/

1. Davis, M.M. & Bjorkman, P.J. T-cell antigen receptor genes and T-cell recognition. *Nature* **334**, 395–402 (1988).
2. Garcia, K.C. *et al.* An αβ T cell receptor structure at 2.5 A and its orientation in the TCR-MHC complex. *Science* **274**, 209–219 (1996).
3. Garboczi, D.N. *et al.* Structure of the complex between human T-cell receptor, viral peptide and HLA-A2. *Nature* **384**, 134–141 (1996).
4. Ding, Y.H., Baker, B.M., Garboczi, D.N., Biddison, W.E. & Wiley, D.C. Four A6-TCR/peptide/HLA-A2 structures that generate very different T cell signals are nearly identical. *Immunity* **11**, 45–56 (1999).
5. Garcia, K.C. *et al.* Structural basis of plasticity in T cell receptor recognition of a self peptide-MHC antigen. *Science* **279**, 1166–1172 (1998).
6. Reinherz, E.L. *et al.* The crystal structure of a T cell receptor in complex with peptide and MHC class II. *Science* **286**, 1913–1921 (1999).
7. Degano, M. *et al.* A functional hot spot for antigen recognition in a superagonist TCR/MHC complex. *Immunity* **12**, 251–261 (2000).
8. Hennecke, J., Carfi, A. & Wiley, D.C. Structure of a covalently stabilized complex of a human αβ T cell receptor, influenza HA peptide and MHC class II molecule, HLA-DR1. *EMBO J.* **19**, 5611–5624 (2000).
9. Reiser, J.B. *et al.* Crystal structure of a T cell receptor bound to an allogeneic MHC molecule. *Nat. Immunol.* **1**, 291–297 (2000).
10. Reiser, J.B. *et al.* A T cell receptor CDR3β loop undergoes conformational changes of unprecedented magnitude upon binding to a peptide/MHC class I complex. *Immunity* **16**, 345–354 (2002).
11. Reiser, J.B. *et al.* CDR3 loop flexibility contributes to the degeneracy of TCR recognition. *Nat. Immunol.* **4**, 241–247 (2003).
12. Luz, J.G. *et al.* Structural comparison of allogeneic and syngeneic T cell receptor-peptide-major histocompatibility complex complexes: a buried alloreactive mutation subtly alters peptide presentation substantially increasing V_β interactions. *J. Exp. Med.* **195**, 1175–1186 (2002).
13. Kjer-Nielsen, L. *et al.* A structural basis for the selection of dominant αβ T cell receptors in antiviral immunity. *Immunity* **18**, 53–64 (2003).
14. Stewart-Jones, G.B., McMichael, A.J., Bell, J.I., Stuart, D.I. & Jones, E.Y. A structural basis for immunodominant human T cell receptor recognition. *Nat. Immunol.* **4**, 657–663 (2003).
15. Garcia, K.C., Teyton, L. & Wilson, I.A. Structural basis of T cell recognition. *Annu. Rev. Immunol.* **17**, 369–397 (1999).
16. Hennecke, J. & Wiley, D.C. T cell receptor-MHC interactions up close. *Cell* **104**, 1–4 (2001).
17. Rudolph, M.G. & Wilson, I.A. The specificity of TCR/pMHC interaction. *Curr. Opin. Immunol.* **14**, 52–65 (2002).
18. van der Merwe, P.A. & Davis, S.J. Molecular interactions mediating T cell antigen recognition. *Annu. Rev. Immunol.* **21**, 659–684 (2003).
19. Willcox, B.E. *et al.* TCR binding to peptide-MHC stabilizes a flexible recognition interface. *Immunity* **10**, 357–365 (1999).
20. Krogsgaard, M. *et al.* Evidence that structural rearrangements and/or flexibility during TCR binding can contribute to T cell activation. *Mol. Cell* **12**, 1367–1378 (2003).
21. Boniface, J.J., Reich, Z., Lyons, D.S. & Davis, M.M. Thermodynamics of T cell receptor binding to peptide-MHC: evidence for a general mechanism of molecular scanning. *Proc. Natl. Acad. Sci. USA* **96**, 11446–11451 (1999).
22. Kersh, G.J., Kersh, E.N., Fremont, D.H. & Allen, P.M. High- and low-potency ligands with similar affinities for the TCR: the importance of kinetics in TCR signaling. *Immunity* **9**, 817–826 (1998).
23. Manning, T.C. *et al.* Alanine scanning mutagenesis of an αβ T cell receptor: mapping the energy of antigen recognition. *Immunity* **8**, 413–425 (1998).
24. Lee, P.U., Churchill, H.R., Daniels, M., Jameson, S.C. & Kranz, D.M. Role of 2CT cell receptor residues in the binding of self- and allo-major histocompatibility complexes. *J. Exp. Med.* **191**, 1355–1364 (2000).
25. Wu, L.C., Tuot, D.S., Lyons, D.S., Garcia, K.C. & Davis, M.M. Two-step binding mechanism for T-cell receptor recognition of peptide MHC. *Nature* **418**, 552–556 (2002).
26. Baker, B.M., Turner, R.V., Gagnon, S.J., Wiley, D.C. & Biddison, W.E. Identification of a crucial energetic footprint on the α1 helix of human histocompatibility leukocyte antigen (HLA)-A2 that provides functional interactions for recognition by tax peptide/HLA-A2-specific T cell receptors. *J. Exp. Med.* **193**, 551–562 (2001).
27. Arstila, T.P. *et al.* A direct estimate of the human αβ T cell receptor diversity. *Science* **286**, 958–961 (1999).
28. Argaet, V.P. *et al.* Dominant selection of an invariant T cell antigen receptor in response to persistent infection by Epstein-Barr virus. *J. Exp. Med.* **180**, 2335–2340 (1994).
29. Callan, M.F. *et al.* Large clonal expansions of CD8$^+$ T cells in acute infectious mononucleosis. *Nat. Med.* **2**, 906–911 (1996).
30. Annels, N.E., Callan, M.F., Tan, L. & Rickinson, A.B. Changing patterns of dominant TCR usage with maturation of an EBV-specific cytotoxic T cell response. *J. Immunol.* **165**, 4831–4841 (2000).
31. Kjer-Nielsen, L. *et al.* The structure of HLA-B8 complexed to an immunodominant viral determinant: peptide-induced conformational changes and a mode of MHC class I dimerization. *J. Immunol.* **169**, 5153–5160 (2002).
32. Kjer-Nielsen, L. *et al.* The 1.5 a crystal structure of a highly selected antiviral T cell receptor provides evidence for a structural basis of immunodominance. *Structure (Camb)* **10**, 1521–1532 (2002).
33. Webb, A.I. *et al.* The structure of H-2K^b and K^{bm8} complexed to a herpes simplex virus determinant: evidence for a conformational switch that governs T cell repertoire selection and viral resistance. *J. Immunol.* **173**, 402–409 (2004).
34. Argaet, V.P. *et al.* Dominant selection of an invariant T cell antigen receptor in response to persistent infection by Epstein-Barr virus. *J. Exp. Med.* **180**, 2335–2340 (1994).
35. Callan, M.F. *et al.* T cell selection during the evolution of CD8$^+$ T cell memory *in vivo*. *Eur. J. Immunol.* **28**, 4382–4390 (1998).
36. Manning, T.C., Parke, E.A., Teyton, L. & Kranz, D.M. Effects of complementarity determining region mutations on the affinity of an αβ T cell receptor: measuring the energy associated with CD4/CD8 repertoire skewing. *J. Exp. Med.* **189**, 461–470 (1999).
37. Speir, J.A. *et al.* Structural basis of 2C TCR allorecognition of H-2Ld peptide complexes. *Immunity* **8**, 553–562 (1998).
38. Callan, M.F. & McMichael, A.J. T cell receptor usage in infectious disease. *Springer Semin. Immunopathol.* **21**, 37–54 (1999).
39. Callan, M.F. *et al.* T cell selection during the evolution of CD8$^+$ T cell memory *in vivo*. *Eur. J. Immunol.* **28**, 4382–4390 (1998).
40. Callan, M.F. *et al.* CD8$^+$ T-cell selection, function, and death in the primary immune response *in vivo*. *J. Clin. Invest.* **106**, 1251–1261 (2000).
41. Mongkolsapaya, J. *et al.* Antigen-specific expansion of cytotoxic T lymphocytes in acute measles virus infection. *J. Virol.* **73**, 67–71 (1999).
42. Callan, M.F. *et al.* Selection of T cell receptor variable gene-encoded amino acids on the third binding site loop: a factor influencing variable chain selection in a T cell response. *Eur. J. Immunol.* **25**, 1529–1534 (1995).
43. Kedzierska, K., Turner, S.J. & Doherty, P.C. Conserved T cell receptor usage in primary and recall responses to an immunodominant influenza virus nucleoprotein epitope. *Proc. Natl. Acad. Sci. USA* **101**, 4942–4947 (2004).
44. Wilson, J.D. *et al.* Oligoclonal expansions of CD8$^+$ T cells in chronic HIV infection are antigen specific. *J. Exp. Med.* **188**, 785–790 (1998).

45. Clackson, T. & Wells, J.A. A hot spot of binding energy in a hormone-receptor interface. *Science* **267**, 383–386 (1995).
46. Wang, Z., Turner, R., Baker, B.M. & Biddison, W.E. MHC allele-specific molecular features determine peptide/HLA-A2 conformations that are recognized by HLA-A2-restricted T cell receptors. *J. Immunol.* **169**, 3146–3154 (2002).
47. Baxter, T.K. *et al.* Strategic mutations in the class I major histocompatibility complex HLA-A2 independently affect both peptide binding and T cell receptor recognition. *J. Biol. Chem.* **279**, 29175–29184 (2004).
48. Burrows, S.R., Khanna, R., Burrows, J.M. & Moss, D.J. An alloresponse in humans is dominated by cytotoxic T lymphocytes (CTL) cross-reactive with a single Epstein-Barr virus CTL epitope: implications for graft-versus-host disease. *J. Exp. Med.* **179**, 1155–1161 (1994).
49. Burrows, S.R. *et al.* Human leukocyte antigen phenotype imposes complex constraints on the antigen-specific cytotoxic T lymphocyte repertoire. *Eur. J. Immunol.* **27**, 178–182 (1997).
50. Zerrahn, J., Held, W. & Raulet, D.H. The MHC reactivity of the T cell repertoire prior to positive and negative selection. *Cell* **88**, 627–636 (1997).
51. Jameson, S.C., Kaye, J. & Gascoigne, N.R. A T cell receptor V_α region selectively expressed in $CD4^+$ cells. *J. Immunol.* **145**, 1324–1331 (1990).
52. Sim, B-C., Zerva, L., Greene, M.I. & Gascoigne, N.R.J. Control of MHC restriction by TcR V_α CDR1 and CDR2. *Science* **273**, 963–966 (1996).
53. Sim, B.C., Wung, J.L. & Gascoigne, N.R. Polymorphism within a TCRAV family influences the repertoire through class I/II restriction. *J. Immunol.* **160**, 1204–1211 (1998).
54. Sha, W.C. *et al.* Selective expression of an antigen receptor on CD8-bearing T lymphocytes in transgenic mice. *Nature* **335**, 271–274 (1988).
55. Garboczi, D.N. & Biddison, W.E. Shapes of MHC restriction. *Immunity* **10**, 1–7 (1999).
56. Patten, P.A. *et al.* The immunological evolution of catalysis. *Science* **271**, 1086–1091 (1996).
57. Clements, C.S. *et al.* The production, purification and crystallization of a soluble heterodimeric form of a highly selected T-cell receptor in its unliganded and liganded state. *Acta Crystallogr. D Biol. Crystallogr.* **58**, 2131–2134 (2002).
58. Parham, P., Barnstable, C.J. & Bodmer, W.F. Use of a monoclonal antibody (W6/32) in structural studies of HLA-A,B,C, antigens. *J. Immunol.* **123**, 342–349 (1979).
59. Panzara, M.A., Gussoni, E., Steinman, L. & Oksenberg, J.R. Analysis of the T cell repertoire using the PCR and specific oligonucleotide primers. *Biotechniques* **12**, 728–735 (1992).